World Journal of Gastroenterology

Online Submissions: http://www.wjgnet.com/esps/
bpgoffice@wjgnet.com
doi:10.3748/wjg.v19.i45.8357

World J Gastroenterol 2013 December 7; 19(45): 8357-8365
ISSN 1007-9327 (print) ISSN 2219-2840 (online)

BRIEF ARTICLE

Added value of hepatobiliary phase gadoxetic acid-enhanced MRI for diagnosing hepatocellular carcinoma in high-risk patients

Sith Phongkitkarun, Kuruwin Limsamutpetch, Penampai Tannaphai, Janjira Jatchavala

Sith Phongkitkarun, Kuruwin Limsamutpetch, Penampai Tannaphai, Janjira Jatchavala, Department of Diagnostic and Therapeutic Radiology, Faculty of Medicine, Ramathibodi Hospital, Mahidol University, Ratchatewi, Bangkok 10400, Thailand

Author contributions: Phongkitkarun S and Limsamutpetch K contributed to the study design, statistical analyses and wrote the first draft; Phongkitkarun S, Limsamutpetch K and Tannaphai P contributed to the data acquisition; Phongkitkarun S and Jatchavala J revised the manuscript.

Correspondence to: Sith Phongkitkarun, MD, Department of Diagnostic and Therapeutic Radiology, Faculty of Medicine, Ramathibodi Hospital, Mahidol University, 270 Rama VI Road, Ratchatewi, Bangkok 10400, Thailand. sith.bkk@gmail.com
Telephone: +66-81-7542780 Fax: +66-2-2011274
Received: May 21, 2013 Revised: August 6, 2013
Accepted: September 16, 2013
Published online: December 7, 2013

Abstract

AIM: To determine the added value of hepatobiliary phase (HBP) gadoxetic acid-enhanced magnetic resonance imaging (MRI) in evaluating hepatic nodules in high-risk patients.

METHODS: The institutional review board approved this retrospective study and waived the requirement for informed consent. This study included 100 patients at high risk for hepatocellular carcinoma (HCC) and 105 hepatic nodules that were larger than 1 cm. A blind review of two MR image sets was performed in a random order: set 1, unenhanced (T1- and T2-weighted) and dynamic images; and set 2, unenhanced, dynamic 20-min and HBP images. The diagnostic accuracy, sensitivity, specificity, positive predictive value (PPV), and negative predictive value (NPV) were compared for the two image sets. Univariate and multivariate analyses were performed on the MR characteristics utilized to diagnose HCC.

RESULTS: A total of 105 hepatic nodules were identified in 100 patients. Fifty-nine nodules were confirmed to be HCC. The diameter of the 59 HCCs ranged from 1 to 12 cm (mean: 1.9 cm). The remaining 46 nodules were benign (28 were of hepatocyte origin, nine were hepatic cysts, seven were hemangiomas, one was chronic inflammation, and one was focal fat infiltration). The diagnostic accuracy significantly increased with the addition of HBP images, from 88.7% in set 1 to 95.5% in set 2 (P = 0.002). In set 1 *vs* set 2, the sensitivity and NPV increased from 79.7% to 93.2% and from 78.9% to 91.8%, respectively, whereas the specificity and PPV were not significantly different. The hypointensity on the HBP images was the most sensitive (93.2%), and typical arterial enhancement followed by washout was the most specific (97.8%). The multivariate analysis revealed that typical arterial enhancement followed by washout, hyperintensity on T2-weighted images, and hypointensity on HBP images were statistically significant MRI findings that could diagnose HCC (P < 0.05).

CONCLUSION: The addition of HBP gadoxetic acid-enhanced MRI statistically improved the diagnostic accuracy in HCCs larger than 1 cm. Typical arterial enhancement followed by washout and hypointensity on HBP images are useful for diagnosing HCC.

Key words: Magnetic resonance imaging; Liver; Gadoxetic acid; Hepatobiliary phase; Hepatocellular carcinoma

Core tip: This study demonstrated the added value of hepatobiliary phase gadoxetic acid-enhanced magnetic resonance imaging (MRI) for diagnosing hepatocellular carcinoma, based on the changes in contrast uptake

on hepatobiliary phase images during hepatocarcinogenesis. The pitfalls of interpreting hepatobiliary phase MRI are important to recognize in obtaining the most accurate results.

Phongkitkarun S, Limsamutpetch K, Tannaphai P, Jatchavala J. Added value of hepatobiliary phase gadoxetic acid-enhanced MRI for diagnosing hepatocellular carcinoma in high-risk patients. *World J Gastroenterol* 2013; 19(45): 8357-8365 Available from: URL: http://www.wjgnet.com/1007-9327/full/v19/i45/8357.htm DOI: http://dx.doi.org/10.3748/wjg.v19.i45.8357

INTRODUCTION

Liver cancer is the second most frequent cause of death in men and the sixth leading cause of death in women worldwide. Southeast Asia is one of the regions with the greatest incidences of liver cancer, and hepatocellular carcinoma (HCC), associated with the hepatitis B virus, accounts for the majority of the cases[1,2].

The therapeutic approach for HCC depends on the accurate diagnosis and identification of HCC lesions, *i.e.*, the number, size, and location of the lesions. In practice, the high prevalence of benign lesions in cirrhotic livers and the variability in HCC imaging characteristics, which depend on differentiation of the state of the disease, render the detection of HCC difficult. Magnetic resonance imaging (MRI), particularly contrast-enhanced dynamic MRI, plays an important role in accurately diagnosing HCC[3]. A study by Forner *et al*[4] reported that the sensitivity and specificity were as high as 62% and 97%, respectively, for detecting HCC with conventional contrast-enhanced dynamic MRI. Nevertheless, undetectable HCC lesions pose a serious issue.

A recent molecular study reported that organic anion transporting polypeptide 8 (OATP8) is expressed in hepatocytes and that OATP8 expression significantly decreases during the multistep process of hepatocarcinogenesis[5]. A newly developed liver-specific contrast agent, gadoxetic acid, is taken up by hepatocytes *via* OATP8 in an *in vitro* study[6]. Therefore, the use of liver-specific contrast-enhanced MRI might provide superior detection and characterization of HCC[7-9].

Gadoxetic acid, or gadolinium ethoxybenzyl diethylenetriamine pentaacetic acid (Gd-EOB-DTPA), has the properties of being both an extracellular gadolinium chelate and a hepatobiliary agent, thus enabling dynamic perfusion imaging, delayed hepatocyte uptake, and biliary excretion. A recent study demonstrated that, compared with conventional contrast-enhanced dynamic and T2-weighted MRI, Gd-EOB-DTPA-enhanced hepatobiliary phase MRI improved HCC detection[3]. However, there are no supportive data for such a benefit in the Thai population, which has a high prevalence of HCC with different risk factors. Because of differences in the population and the nature of the disease, we performed a study to determine the added value of Gd-EOB-DTPA-enhanced hepatobiliary phase MRI for diagnosing HCC in high-risk patients.

Table 1 Demographic characteristics of the study population (n = 100) n (%)

Variables	Results
Age (mean ± SD; range, yr)	59.5 ± 11.4 (range 27-89)
Sex (male:female)	71:29
Risk factors for HCC	
Chronic HBV infection	20 (20)
Chronic HCV infection	2 (2)
Hepatitis B-related cirrhosis	45 (45)
Hepatitis C-related cirrhosis	16 (16)
Alcoholic cirrhosis	9 (9)
Nonalcoholic steatohepatitis	6 (6)
Only high serum AFP levels	2 (2)
Child-Pugh score	
A	94 (94)
B	5 (5)
C	1 (1)
Alpha-fetoprotein (mean ± SD; range, ng/mL)	111.6 ± 935.1 (range 0.98-8973)
< 20	84 (84)
20-200	5 (5)
> 200	3 (3)
Total bilirubin (mean ± SD; range, mg/dL)	1.43 ± 2.5 (range 0.2-17.1)

HBV: Hepatitis B virus; HCV: Hepatitis C virus; HCC: Hepatocellular carcinoma; AFP: Alpha-fetoprotein.

MATERIALS AND METHODS

Patient selection and reference standards

This retrospective study was approved by our institutional review board, which waived the informed consent requirement. Between January 2010 and July 2010, 100 consecutive patients (mean age: 59.5 years old; range: 27-89 years), consisting of 71 men (mean age: 59.4 years; range: 27-89 years) and 29 women (mean age: 59.6 years old; range: 36-81 years), were registered as high-risk patients with HCC and underwent Gd-EOB-DTPA-enhanced MRI. The high-risk patients included those with chronic viral hepatitis infections (HBV or HCV infection), liver cirrhosis, or elevated serum alpha-fetoprotein (AFP) levels. Among the 100 patients, 76 had liver cirrhosis. Forty-five patients had hepatitis B-related cirrhosis, 16 had hepatitis C-related cirrhosis, nine had alcoholic cirrhosis, six had nonalcoholic steatohepatitis, 22 had a chronic hepatitis infection (20 with chronic hepatitis B and two with chronic hepatitis C), and the remaining two patients only presented with abnormal serum AFP. The Child-Pugh score was calculated for all of the patients within 60 d of the MRI scan (Table 1).

The reference standard for diagnosing HCC was classified as follows: based on pathologically proven HCC (by surgical specimen or percutaneous biopsy); by lipiodol staining after transhepatic arterial chemoembolization (TACE); or on the basis of progression of the disease on follow-up computed tomography (CT) or MRI performed at least 6 mo after the initial imaging.

Table 2 1.5-T and 3.0-T magnetic resonance pulse sequence parameters

Parameters	Double-echo T1-weighted gradient echo		Respiratory-triggered fast-spin T2-weighted		T1-weighted Gd-EOB-DTPA-enhanced	
	1.5-T	3.0-T	1.5-T	3.0-T	1.5-T	3.0-T
Matrix	256 × 192	228 × 136	320 × 224	320 × 188	256 × 192	180 × 163
Section thickness (mm)	6-8	6	4	6	2-3	4
Intersection gap (mm)	2	2	1	2	-	-
TR (ms)	180-220	150-250	2000-4000	2500-3500	4.2	2.8
TE (ms)	2.3-4.6	1.15-2.3	60	65-85	2	1.4
Flip angle (degrees)	80	70	90	120	12	10
Reduction factor	2	2	2	2	2	2

Gd-EOB-DTPA: Gadolinium ethoxybenzyl diethylenetriaminepentaacetic.

MRI methods

All of the MRI studies were performed with a 1.5-T system (Signa HDxt; GE Healthcare, Milwaukee, Wisconsin, United States) and a 3.0-T system (Intera Achieva; Philips Medical Systems, Best, The Netherlands) with phased-array coils. All of the images were obtained on the axial plane. The field of view (32-40 cm × 32-40 cm) was adjusted for each patient. The MR protocol consisted of a double-echo T1-weighted gradient-echo sequence (in-phase and opposed-phase), a respiratory-triggered fast-spin T2-weighted sequence, and a contrast-enhanced dynamic sequence. The parameters for all of the sequences are presented in Table 2. For the contrast-enhanced dynamic MR images, Gd-EOB-DTPA was administered at 0.025 mmol per kilogram of body weight at 2 mL per second, followed by a 10-mL saline flush. After administering the contrast, early arterial phase (25-30 s), late arterial phase (45-50 s), portal venous phase (65-70 s), equilibrium phase (5 min), and additional hepatobiliary phase (after 20 min) images were obtained.

MR image analysis

Two sets of MR images were reviewed by an experienced gastrointestinal radiologist (S.P.) in a random order. The observer was blinded to the patient history, the findings from other imaging modalities, treatments, outcomes, and the final diagnoses. Set 1 of the MR images contained unenhanced (pre-contrast T1- and T2-weighted images) and Gd-EOB-DTPA-enhanced dynamic images (arterial, portal venous, and 5-min equilibrium phases); set 2 consisted of unenhanced, Gd-EOB-DTPA-enhanced dynamic, and 20-min hepatobiliary phase images. The MR images in set 2 were obtained at least 1 mo after finishing the reviews of all of the MR images in set 1. A diagnosis of HCC met at least one of the following criteria: (1) a liver nodule 1 cm or larger, with increased enhancement on arterial phase images and washout on portal venous or equilibrium phase images[10]; or (2) a hypervascular liver nodule 1 cm or larger, with no uptake on 20-min hepatobiliary phase Gd-EOB-DTPA-enhanced MR images[11].

The observer recorded the possibility of HCC for each dominant lesion (defined as 1 cm or larger) using a four-point confidence rating scale: (1) unlikely to be HCC; (2) a concerning nodule; (3) probably HCC; and (4) definitely HCC. A score of 0 was recorded when the observer did not find any dominant lesions. Lesions that received a score of 3 or 4 were classified as positive for HCC in later analyses. The size and location of each lesion were clearly documented using liver segmental anatomy, defined by Couinaud classification and MR characteristics (in-phase, opposed-phase, T2-weighted, arterial phase, portal venous phase, 5-min equilibrium phase, and 20-min hepatobiliary phase images, which were only obtained in set 2). All of the MR images were reviewed with Picture Archiving and Communications System (PACS) and Digital Imaging and Communications in Medicine Conformance (Synapse, version 3.2.0, FUJIFILM Medical Systems United Stated's Synapse® PACS system, Stamford, Connecticut, United States).

Statistical analysis

Statistical analyses were performed using statistical software (SPSS, version 17.0.1, SPSS, Chicago, Illinois, United States). Descriptive statistics were calculated for all of the clinical variables and for those evaluated on the MR images. For continuous data (age, AFP level, total bilirubin level, and lesion size), the means, SDs, and ranges were calculated. Descriptive statistics, such as raw numbers and percentages, were determined for categorical data. An alternative free-response receiver operating characteristic analysis was performed on the confidence rating scale of the observer. The area under the alternative free-response receiver operating characteristic curve (A_z) was utilized to determine the diagnostic accuracy of detecting HCC in each image set and according to lesion size (1-2 cm or larger than 2 cm). Sensitivity, specificity, positive predictive values (PPVs), and negative predictive values (NPVs) were calculated for the two MR image sets.

The relationships between each MRI variable and the presence of an HCC lesion were tested *via* univariate analysis. Significant variables identified by the univariate analysis were integrated into the logistic regression model for the multivariate analysis. The MRI variables with significant associations in the multivariate analysis were regarded as significant predictors of the presence of HCC. All of the statistical tests were two-tailed, and a P value of < 0.05 indicated statistical significance.

RESULTS

A total of 105 hepatic nodules were identified in 100 patients. Fifty-nine nodules were confirmed to be HCC by

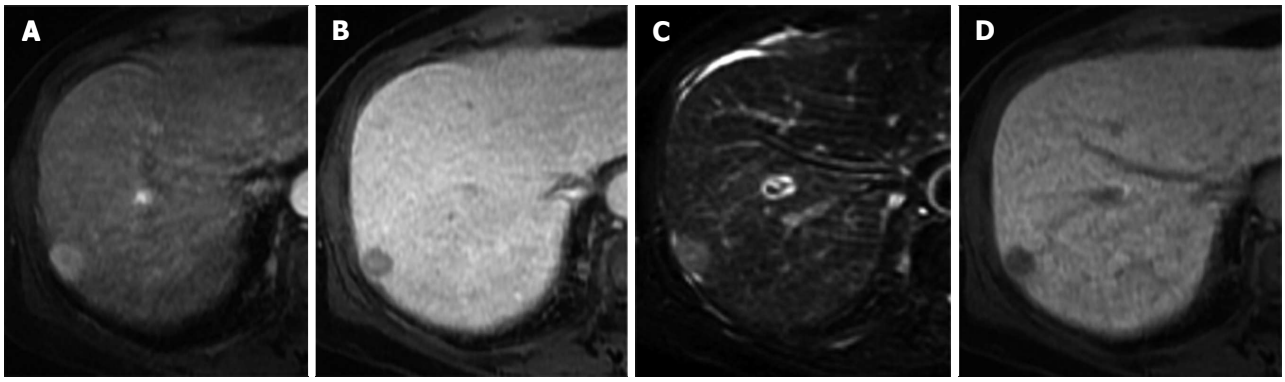

Figure 1 Magnetic resonance images from a 77-year-old woman with hepatitis B virus cirrhosis. A liver nodule at segment Ⅶ was surgically confirmed as hepatocellular carcinoma. Gadolinium ethoxybenzyl diethylenetriaminepentaacetic -enhanced magnetic resonance (MR) arterial phase images depicting a 1.9-cm arterial enhanced nodule (A) with rapid washout on the equilibrium phase image (B). C: Hyperintensity on a T2-weighted MR image; D: Hypointensity on a 20-min hepatobiliary phase image.

Table 3 Diagnostic accuracy of diagnosing hepatocellular carcinoma using conventional dynamic magnetic resonance imaging or conventional dynamic magnetic resonance imaging with hepatobiliary phase images

	Conventional dynamic MRI	Conventional dynamic MRI + HBP	*P* value
All lesions	88.7%	95.5%	0.002
Lesions 1-2 cm	86.7%	94.0%	0.008
Lesions > 2 cm	94.4%	100%	0.145

MRI: Magnetic resonance imaging; HBP: Hepatobiliary phase.

Table 4 Sensitivity, specificity, and positive and negative predictive values for diagnosing hepatocellular carcinoma using conventional dynamic magnetic resonance imaging or conventional dynamic magnetic resonance imaging with hepatobiliary phase images

	Conventional dynamic MRI	95%CI	Conventional dynamic MRI + HBP	95%CI
Sensitivity	79.7%	67.2-89.0	93.2%	83.5-98.1
Specificity	97.8%	85.5-99.9	97.8%	88.5-99.9
Positive predictive value	97.9%	88.9-99.9	98.2%	90.4-100.0
Negative predictive value	78.9%	66.1-88.6	91.8%	80.4-97.7

MRI: Magnetic resonance imaging; HBP: Hepatobiliary phase.

pathologic examination of surgical resection or percutaneous biopsy specimens (n = 23), by lipiodol staining after TACE (n = 30), or on the basis of disease progression on follow-up CT or MRI at least 6 mo after the initial imaging (n = 6; mean: 11.9 mo). The diameter of the 59 HCCs ranged from 1 to 12 cm (mean: 1.9 cm). The remaining 46 nodules were benign (28 were of hepatocyte origin, nine were hepatic cysts, seven were hemangiomas, one was chronic inflammation, and one was focal fat infiltration). Four of the 46 nodules were pathologically confirmed as benign lesions (two were regenerative nodules, one was a cirrhotic nodule, and one was a hemangioma), and 42 nodules were considered benign because they decreased or remained unchanged in size on the last follow-up CT, or MRI (mean: 22.1 mo).

The diagnostic accuracy of diagnosing HCC in the two image sets is presented in Table 3. The diagnostic accuracy of the combination of unenhanced, Gd-EOB-DTPA-enhanced dynamic, and 20-min hepatobiliary phase images (set 2, 95.5%) was significantly greater than that of the unenhanced and Gd-EOB-DTPA-enhanced dynamic images (set 1, 88.7%) (P = 0.002; Figure 1). For 1- to 2-cm lesions, the diagnostic accuracy significantly improved from 86.7% in set 1 to 94.0% in set 2 (P = 0.008), whereas there was no statistical improvement for lesions > 2 cm (94.4% in set 1 and 100% in set 2; P = 0.145).

The sensitivity, specificity, PPVs, and NPVs for the two image sets are presented in Table 4. The addition of 20-min hepatobiliary phase images increased the sensitivity from 79.7% (95%CI: 67.2-89) to 93.2% (95%CI: 83.5-98.1). The specificity of both sets was 97.8% (95%CI: 85.5-99.9). The addition of 20-min hepatobiliary phase images increased the positive and NPVs from 97.9% (95%CI: 88.9-99.9) to 98.2% (95%CI: 90.4-100) and from 78.9% (95%CI: 66.1-88.6) to 91.8% (95%CI: 80.4-97.7), respectively.

The sensitivity, specificity, PPVs, and NPVs of each MRI characteristic utilized to diagnose HCC were as follows: (1) fat metamorphosis: 16.9% (95%CI: 8.4-29), 95.7% (95%CI: 85.2-99.5), 83.3% (95%CI: 51.6-97.9),

Table 5 Sensitivity, specificity, and positive and negative predictive values for diagnosing hepatocellular carcinoma based on magnetic resonance imaging findings after excluding cysts and hemangiomas (n = 89)

MRI findings	Sensitivity (%)	Specificity (%)	Positive predictive value (%)	Negative predictive value (%)
Fat metamorphosis	16.9 (8.4-29.0)	93.3 (77.9-99.2)	83.3 (51.6-97.9)	36.4 (25.7-48.1)
Hyperintensity on T2-weighted images	66.1 (52.6-77.9)	93.3 (77.9-99.2)	95.1 (83.5-99.4)	58.3 (43.2-72.4)
Arterial enhancement	88.1 (77.1-95.1)	70.0 (50.6-85.3)	85.2 (73.8-93.0)	75.0 (55.1-89.3)
Arterial enhancement and washout on venous or equilibrium phase	79.7 (67.2-89.0)	96.7 (82.8-99.9)	97.9 (88.9-99.9)	70.7 (54.5-83.9)
Hypointensity on 20-min hepatobiliary phase	93.2 (83.5-98.1)	53.3 (34.3-71.7)	79.7 (68.3-88.4)	80.0 (56.3-94.3)
Arterial enhancement and no/partial uptake on 20-min hepatobiliary phase	83.1 (71.0-91.6)	93.3 (77.9-99.2)	96.1 (86.5-99.5)	73.7 (56.9-86.6)

MRI: Magnetic resonance imaging.

Table 6 Results of the univariate analysis of the magnetic resonance imaging findings for the diagnosis of hepatocellular carcinoma n (%)

MRI findings	All lesions (n = 105)			Lesions excluding cysts and hemangiomas (n = 89)		
	HCC (n = 59)	Not HCC (n = 46)	P value	HCC (n = 59)	Not HCC (n = 30)	P value
Fat metamorphosis	10 (16.9)	2 (4.3)	0.061	10 (16.9)	2 (6.7)	0.190
Hyperintensity on T2-weighted images	39 (66.1)	18 (39.1)	0.007	39 (66.1)	2 (6.7)	< 0.001
Arterial enhancement	52 (88.1)	15 (32.6)	< 0.001	52 (88.1)	9 (30)	< 0.001
Arterial enhancement and washout on venous or equilibrium phase images	47 (79.7)	1 (2.2)	< 0.001	47 (79.7)	1 (3.3)	< 0.001
Hypointensity on 20-min hepatobiliary phase images	55 (93.2)	30 (65.2)	0.001	55 (93.2)	14 (46.7)	< 0.001
Arterial enhancement and no/partial uptake on 20-min hepatobiliary phase images	49 (83.1)	8 (17.4)	< 0.001	49 (83.1)	2 (6.7)	< 0.001

HCC: Hepatocellular carcinoma. MRI: Magnetic resonance imaging.

Table 7 Results of the multivariate analysis of the magnetic resonance imaging findings for diagnosing hepatocellular carcinoma

MRI findings	All lesions (n = 105)			Lesions excluding cysts and hemangiomas (n = 89)		
	OR	95%CI	P value	OR	95%CI	P value
Hyperintensity on T2-weighted images	1.1	0.3-4.3	0.86	12.6	1.8-87.8	0.01
Arterial enhancement	1.8	0.4-7.0	0.42	3.5	0.5-22.8	0.18
Arterial enhancement and washout on venous or equilibrium phase images	102.0	10.3-1012.4	< 0.001	16.9	1.3-221.1	0.03
Hypointensity on 20-min hepatobiliary phase images	1.8	0.4-8.6	0.48	6.7	1.1-41.9	0.04

MRI: Magnetic resonance imaging.

and 47.3% (95%CI: 36.9-57.9); (2) hyperintensity on T2-weighted images: 66.1% (52.6-77.9), 60.9% (45.4-74.9), 68.4% (54.8-80.1), and 58.3% (43.2-72.4); (3) arterial enhancement: 88.1% (77.1-95.1), 67.4% (52.0-80.5), 77.6% (65.8-86.9), and 81.6% (65.7-92.3); (4) arterial enhancement and washout on venous or equilibrium phase images: 79.7% (67.2-89.0), 97.8% (88.5-99.9), 97.9% (88.9-99.9), and 78.9% (66.1-88.6); (5) hypointensity on 20-min hepatobiliary phase images: 93.2% (83.5-98.1), 34.8% (21.4-50.2), 64.7% (53.6-74.8), and 80% (56.3-94.3); and (6) arterial enhancement and no or partial uptake on 20-min hepatobiliary phase images: 83.1% (71.0-91.6), 82.6% (68.6-92.2), 86% (74.2-93.7), and 79.2% (65.0-89.5). The MRI finding with the greatest sensitivity (93.2%) for detecting HCC was hypointensity on the 20-min hepatobiliary phase images, and the greatest specificity (97.8%) for detecting HCC occurred with typical arterial enhancement and washout on venous or equilibrium phase images. Excluding cysts and hemangiomas, the specificity of diagnosing HCC was greater for hyperintense T2-weighted images and for hypointensities on hepatobiliary phase images (Table 5).

Table 6 summarizes the results of the univariate analysis of the ability of the MRI findings in the two groups to diagnose HCC, as well as the results after excluding cysts and hemangiomas. Although almost all of the MRI features were statistically significant in the univariate analysis, the multivariate analysis revealed that only the arterial enhancement and washout on venous or equilibrium phase images were statistically significant MRI findings (P < 0.001; OR = 102.0; 95%CI: 10.3-1012.4; Table 7). Furthermore, typical arterial enhancement followed by washout on venous or equilibrium phases, hyperintensity on T2-weighted images, and hypointensity on 20-min hepatobiliary phase images were statistically significant MRI findings, after excluding cysts and hemangiomas.

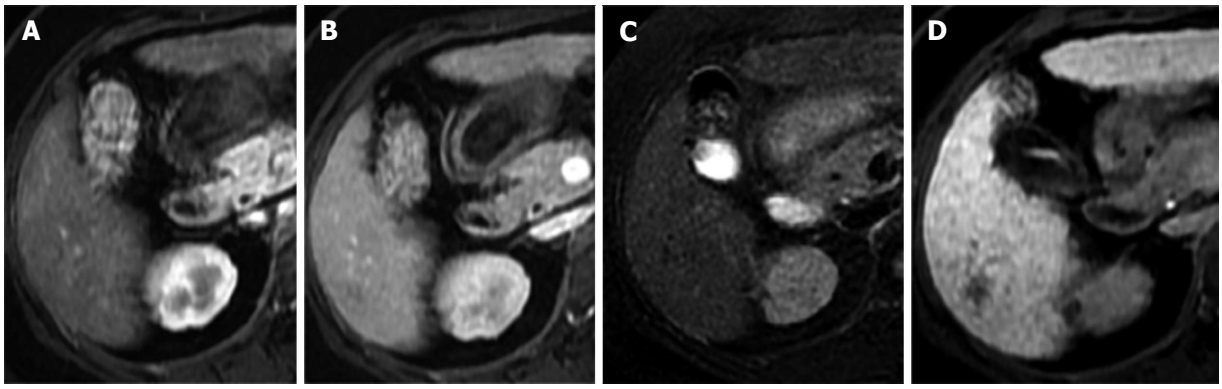

Figure 2 Magnetic resonance images from a 59-year-old woman with hepatocellular carcinoma at hepatic segment VI. This patient underwent transhepatic arterial chemoembolization, and the 6-wk follow-up computerized tomography scan revealed lipiodol staining in the lesion. A and B: Arterial phase and portal venous phase images; C: T2-weighted magnetic resonance image with no definite focal lesion; D: The hepatobiliary phase image revealed a 1.0-cm discrete nodule that was not visible on the dynamic or T2-weighted images.

DISCUSSION

Our study demonstrated that adding hepatobiliary phase Gd-EOB-DTPA-enhanced MRI significantly improved the accuracy of diagnosing HCC. The significant improvement was particularly apparent for small lesions (1-2 cm in diameter). No significant differences were observed for lesions larger than 2 cm in diameter. This finding could be explained by most large HCCs being unequivocally diagnosed based on clearly enhanced characteristics using conventional dynamic MRI. Smaller HCCs sometimes exhibit atypical enhancement characteristics. Therefore, the inclusion of the hepatobiliary phase provided more information for including or excluding the diagnosis of HCC for small nodules. However, other important information for diagnosing HCC was still based on conventional dynamic MRI.

Sensitivity increased with the addition of hepatobiliary phase images, whereas specificity did not change. The inclusion of hepatobiliary phase images allowed subtle abnormalities present in other sequences to be visualized more clearly. The results of our study agreed with those of recent reports in terms of the improvement of diagnostic performance, the characterization of HCC, and the dismissal of pseudolesions[3,10,12-14]. In our study, adding the hepatobiliary phase images increased lesion detection by eight HCCs (13.5%), compared with conventional dynamic MRI (Figure 2).

Our study also highlighted other characteristic MRI findings that were involved in diagnosing HCC. Fat metamorphosis, which can be seen with chemical shift GRE imaging, was present in 10 of 59 HCCs (16.9%) with high specificity (93.3%). Two of the 46 benign lesions (4.3%) with fat components were histologically confirmed to be regenerative nodules in the background of cirrhosis and focal fat infiltration in normal livers. The results were similar to those in the study by Martín *et al*[15]. The presence of various fat alterations might be a significant morphological marker for malignant transformation from adenomatous hyperplasia to HCC, although it occurs rarely and can be present in benign hepatic nodules in cirrhotic patients[15,16].

A recent study demonstrated that T2-weighted images did not provide additional diagnostic value in detecting and characterizing focal lesions. The heterogeneity and hyperintense fibrotic septa and bridges in cirrhotic liver parenchyma can obscure moderately hyperintense HCCs on T2-weighted images, and 42%-53% of HCCs can also be isointense to hypointense on T2-weighted images[17]. In this study, however, the specificity improved with the addition of T2-weighted images after excluding cysts and hemangiomas, and T2-weighted images had the greatest sensitivity among all of the tests, with an odds ratio statistically different from 1 for differentiating HCC from benign lesions larger than 1 cm; these results were similar to those of previous reports[18,19].

In 2010, the American Association for the Study of Liver Diseases guidelines for 1- to 2-cm HCCs were changed to require the visualization of a typical enhancement pattern using only one contrast-enhanced imaging technique[10]. In our series, a typical enhancement pattern was observed in 47 of 59 HCC lesions (79.7%) and in one of 30 benign lesions (3.3%); this benign lesion was determined by tissue biopsy to be a regenerating nodule. In our study, 12 of 59 HCC lesions (20.3%) had no typical arterial enhancement or washout on portal venous or equilibrium phase images, and these lesions were classified as well-differentiated HCCs (Figure 3); one had a motion artifact that resulted in a technical error. A recent study by Witjes *et al*[20] demonstrated a strong association between the presence of washout on dynamic MRI and moderately to poorly differentiated HCC.

The majority of the HCCs in our study (55 lesions, 93.2%) had no uptake or partial uptake on the hepatobiliary phase images. Only four HCC lesions (6.8%) were iso- or hyperintense on the hepatobiliary phase images. Fortunately, three-quarters were scored as probably HCC based on the presence of a hypointense capsule, even without the typical enhancement pattern (Figure 3). Two lesions were histologically confirmed to be well-differentiated HCCs. The diminished obviousness of these well-differentiated lesions on hepatobiliary phase

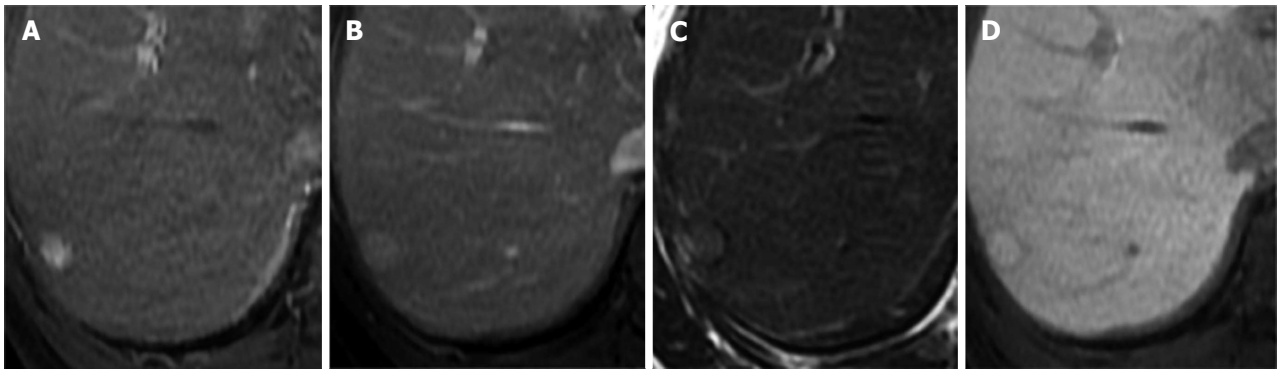

Figure 3 Magnetic resonance images from a 54-year-old man with a 1.4-cm hepatocellular carcinoma with liver-specific contrast uptake at segment Ⅶ. This nodule was confirmed by tissue biopsy to be a well-differentiated hepatocellular carcinoma. Arterial enhanced nodule (A) without washout on the portal venous (B) phase images; C: A slightly hyperintense nodule with a hypointense capsule on a T2-weighted magnetic resonance image; D: Hepatobiliary phase image illustrating the hyperintense nodule.

images might have been related to residual hepatocyte activity within the lesions, enabling the delayed uptake of the contrast material[3]. Another possible cause of diminished obviousness on the hepatobiliary phase images was impaired hepatic function or hyperbilirubinemia, which can affect the hepatocyte uptake of the contrast agent in the liver parenchyma[21]. However, all of the false-negative cases in our study that demonstrated iso- or hyperintensity on the hepatobiliary phase images had normal bilirubin levels. A recent study by Kim *et al*[22] reported that 10% of HCCs were hyperintense on hepatobiliary phase images, and most of the hyperintense HCCs were either well differentiated or moderately differentiated.

A variety of benign hepatic lesions can appear hypointense on hepatobiliary-phase MRI because of the following causes: (1) a lack of functional hepatocytes in the lesion; (2) damage to the functional hepatocytes from infection or inflammation; and (3) impairment of the biliary function of the lesion[23]. In this study, hepatic cysts and hemangiomas accounted for most of the benign hypointense lesions on hepatobiliary phase images. To reduce false-positive findings, hepatobiliary phase imaging should be considered an adjunct method, rather than the sole method, for diagnosing HCC. By excluding benign hepatic cysts and hemangiomas, the arterial enhancement with hypointensity on hepatobiliary phase images had high diagnostic accuracy, comparable to the typical enhancement pattern for HCC (sensitivity: 83.1% *vs* 79.7%; specificity: 93.3% *vs* 96.7%). However, false-positive cases accounted for one (3.3%) typical enhancement pattern and two (6.7%) arterial enhancement patterns with hypointensity on hepatobiliary phase images. These cases were hypothesized to be dysplastic nodules that had stable appearances on imaging.

Several limitations of this study should be addressed. First, the retrospective nature introduced the possibility of selection bias, although we attempted to avoid bias by recruiting consecutively registered patients who met the inclusion criteria. Second, not all of the lesions were confirmed pathologically, which could have introduced verification bias. Histopathology was obtained for 23 of 59 (39%) HCC lesions and four of 46 (8.7%) benign lesions. However, we attempted to avoid this factor by extending the follow-up period to confirm the benign diagnoses (mean: 22.2 mo). Additionally, lesions smaller than 1 cm in diameter were not included in the study. Third, because we had only one observer scoring the images, testing inter-observer reliability was not feasible, and observer bias could have occurred. Finally, our findings might not reflect a direct comparison between imaging with an extracellular contrast agent and a liver-specific hepatobiliary agent. Hepatobiliary enhancement can begin as early as the first pass (the portal venous phase); therefore, it can be difficult to define clearly which phase is the most important for diagnosing HCC: the contrast-enhanced dynamic images or the hepatobiliary phase images.

In a conclusions, The addition of hepatobiliary phase imaging after the intravenous injection of Gd-EOB-DTPA significantly improved diagnostic accuracy in detecting HCC in high-risk patients. Typical arterial enhancement followed by washout, hyperintensity on T2-weighted images, and hypointensity on 20-min hepatobiliary phase images were useful for diagnosing HCCs larger than 1 cm.

COMMENTS

Background

Dynamic imaging plays an important role in diagnosis of hepatocellular carcinoma (HCC), which is based on typical enhancement characteristics. For years, rapid arterial enhancement and rapid washout pattern in dynamic contrast study is accepted as one of diagnostic criteria without tissue pathology. However, there are still limitations in term of sensitivity and specificity, particular in small lesions or during early phase of hepatocarcinogenesis. The newly developed hepatocyte-specific contrast [gadolinium ethoxybenzyl diethylenetriaminepentaacetic (Gd-EOB-DTPA)] that has ability to evaluate both enhancement characteristics and hepatocyte function could have a potential in improving diagnostic accuracy.

Research frontiers

The change of organic anion transporting polypeptide 8 expression in hepatocytes during the multistep process of hepatocarcinogenesis could be imaged by a newly developed hepatocyte-specific contrast agent, gadoxetic acid, on dynamic magnetic resonance imaging (MRI). The use of hepatocyte-specific contrast-enhanced MRI provides superior detection and characterization of HCC.

Innovations and breakthroughs

Adding hepatobiliary phase Gd-EOB-DTPA-enhanced MRI significantly improved the accuracy of diagnosing HCC. The significant improvement is apparent for small lesions (1-2 cm in diameter), for including or excluding the diagnosis of HCC, particular when the nodules exhibit atypical enhancement characteristics. The specificity can be improved with the addition of T2-weighted images after excluding cysts and hemangiomas during interpretation.

Applications

A typical enhancement pattern on dynamic imaging for diagnosing HCC has limited sensitivity, particular for small lesions. Therefore, the addition of hepatobiliary phase imaging after the intravenous injection of Gd-EOB-DTPA will improve diagnostic accuracy in detecting HCC. However, a variety of benign hepatic lesions can appear hypointense on hepatobiliary-phase MRI. To get the best diagnostic accuracy, the hepatobiliary phase imaging should be interpreted in together with early dynamic phases and T2-weighted images.

Peer review

Gadoxetic acid (Gd-EOB-DTPA)-enhanced MRI of the liver has certain advantages over other imaging modalities in the detection and characterization of HCC in the high-risk liver. Hepatobiliary phase images obtained after Gd-EOB-DTPA-enhanced MRI imaging may improve diagnosis of HCC and assist in surgical planning. This study aims to the added value of hepatobiliary phase Gadoxetic acid-enhanced MRI for diagnosis of HCC by the fact that there would be the changes of hepatocyte-specific contrast uptake on hepatobiliary phase during hepatocarcinogenesis and the interpretation's pitfalls of hepatobiliary phase MRI is also important to know for getting the most accurate result.

REFERENCES

1 **Jemal A**, Bray F, Center MM, Ferlay J, Ward E, Forman D. Global cancer statistics. *CA Cancer J Clin* 2011; **61**: 69-90 [PMID: 21296855 DOI: 10.3322/caac.20107]

2 **Vatanasapt V**, Sriamporn S, Vatanasapt P. Cancer control in Thailand. *Jpn J Clin Oncol* 2002; **32** Suppl: S82-S91 [PMID: 11959881 DOI: 10.1093/jjco/hye134]

3 **Ahn SS**, Kim MJ, Lim JS, Hong HS, Chung YE, Choi JY. Added value of gadoxetic acid-enhanced hepatobiliary phase MR imaging in the diagnosis of hepatocellular carcinoma. *Radiology* 2010; **255**: 459-466 [PMID: 20413759 DOI: 10.1148/radiol.10091388]

4 **Forner A**, Vilana R, Ayuso C, Bianchi L, Solé M, Ayuso JR, Boix L, Sala M, Varela M, Llovet JM, Brú C, Bruix J. Diagnosis of hepatic nodules 20 mm or smaller in cirrhosis: Prospective validation of the noninvasive diagnostic criteria for hepatocellular carcinoma. *Hepatology* 2008; **47**: 97-104 [PMID: 18069697 DOI: 10.1002/hep.21966]

5 **Kitao A**, Matsui O, Yoneda N, Kozaka K, Shinmura R, Koda W, Kobayashi S, Gabata T, Zen Y, Yamashita T, Kaneko S, Nakanuma Y. The uptake transporter OATP8 expression decreases during multistep hepatocarcinogenesis: correlation with gadoxetic acid enhanced MR imaging. *Eur Radiol* 2011; **21**: 2056-2066 [PMID: 21626360 DOI: 10.1007/s00330-011-2165-8]

6 **Leonhardt M**, Keiser M, Oswald S, Kühn J, Jia J, Grube M, Kroemer HK, Siegmund W, Weitschies W. Hepatic uptake of the magnetic resonance imaging contrast agent Gd-EOB-DTPA: role of human organic anion transporters. *Drug Metab Dispos* 2010; **38**: 1024-1028 [PMID: 20406852 DOI: 10.1124/dmd.110.032862]

7 **Halavaara J**, Breuer J, Ayuso C, Balzer T, Bellin MF, Blomqvist L, Carter R, Grazioli L, Hammerstingl R, Huppertz A, Jung G, Krause D, Laghi A, Leen E, Lupatelli L, Marsili L, Martin J, Pretorius ES, Reinhold C, Stiskal M, Stolpen AH. Liver tumor characterization: comparison between liver-specific gadoxetic acid disodium-enhanced MRI and biphasic CT--a multicenter trial. *J Comput Assist Tomogr* 2006; **30**: 345-354 [PMID: 16778605 DOI: 10.1097/00004728-200605000-00001]

8 **Hammerstingl R**, Huppertz A, Breuer J, Balzer T, Blakeborough A, Carter R, Fusté LC, Heinz-Peer G, Judmaier W, Laniado M, Manfredi RM, Mathieu DG, Müller D, Mortelè K, Reimer P, Reiser MF, Robinson PJ, Shamsi K, Strotzer M, Taupitz M, Tombach B, Valeri G, van Beers BE, Vogl TJ. Diagnostic efficacy of gadoxetic acid (Primovist)-enhanced MRI and spiral CT for a therapeutic strategy: comparison with intraoperative and histopathologic findings in focal liver lesions. *Eur Radiol* 2008; **18**: 457-467 [PMID: 18058107 DOI: 10.1007/s00330-007-0716-9]

9 **Kim SH**, Kim SH, Lee J, Kim MJ, Jeon YH, Park Y, Choi D, Lee WJ, Lim HK. Gadoxetic acid-enhanced MRI versus triple-phase MDCT for the preoperative detection of hepatocellular carcinoma. *AJR Am J Roentgenol* 2009; **192**: 1675-1681 [PMID: 19457834 DOI: 10.2214/AJR.08.1262]

10 **Bruix J**, Sherman M. Management of hepatocellular carcinoma: an update. *Hepatology* 2011; **53**: 1020-1022 [PMID: 21374666 DOI: 10.1002/hep.24199]

11 **Kudo M**, Izumi N, Kokudo N, Matsui O, Sakamoto M, Nakashima O, Kojiro M, Makuuchi M. Management of hepatocellular carcinoma in Japan: Consensus-Based Clinical Practice Guidelines proposed by the Japan Society of Hepatology (JSH) 2010 updated version. *Dig Dis* 2011; **29**: 339-364 [PMID: 21829027 DOI: 10.1159/000327577]

12 **Golfieri R**, Renzulli M, Lucidi V, Corcioni B, Trevisani F, Bolondi L. Contribution of the hepatobiliary phase of Gd-EOB-DTPA-enhanced MRI to Dynamic MRI in the detection of hypovascular small (≤ 2 cm) HCC in cirrhosis. *Eur Radiol* 2011; **21**: 1233-1242 [PMID: 21293864 DOI: 10.1007/s00330-010-2030-1]

13 **Huppertz A**, Balzer T, Blakeborough A, Breuer J, Giovagnoni A, Heinz-Peer G, Laniado M, Manfredi RM, Mathieu DG, Mueller D, Reimer P, Robinson PJ, Strotzer M, Taupitz M, Vogl TJ. Improved detection of focal liver lesions at MR imaging: multicenter comparison of gadoxetic acid-enhanced MR images with intraoperative findings. *Radiology* 2004; **230**: 266-275 [PMID: 14695400 DOI: 10.1148/radiol.2301020269]

14 **Chou CT**, Chen YL, Su WW, Wu HK, Chen RC. Characterization of cirrhotic nodules with gadoxetic acid-enhanced magnetic resonance imaging: the efficacy of hepatocyte-phase imaging. *J Magn Reson Imaging* 2010; **32**: 895-902 [PMID: 20882620 DOI: 10.1002/jmri.22316]

15 **Martín J**, Sentís M, Zidan A, Donoso L, Puig J, Falcó J, Bella R. Fatty metamorphosis of hepatocellular carcinoma: detection with chemical shift gradient-echo MR imaging. *Radiology* 1995; **195**: 125-130 [PMID: 7892452]

16 **Eguchi A**, Nakashima O, Okudaira S, Sugihara S, Kojiro M. Adenomatous hyperplasia in the vicinity of small hepatocellular carcinoma. *Hepatology* 1992; **15**: 843-848 [PMID: 1314770 DOI: 10.1002/hep.1840150516]

17 **Hussain HK**, Syed I, Nghiem HV, Johnson TD, Carlos RC, Weadock WJ, Francis IR. T2-weighted MR imaging in the assessment of cirrhotic liver. *Radiology* 2004; **230**: 637-644 [PMID: 14739306 DOI: 10.1148/radiol.2303020921]

18 **Bashir MR**, Gupta RT, Davenport MS, Allen BC, Jaffe TA, Ho LM, Boll DT, Merkle EM. Hepatocellular carcinoma in a North American population: does hepatobiliary MR imaging with Gd-EOB-DTPA improve sensitivity and confidence for diagnosis? *J Magn Reson Imaging* 2013; **37**: 398-406 [PMID: 23011874 DOI: 10.1002/jmri.23818]

19 **Kim JE**, Kim SH, Lee SJ, Rhim H. Hypervascular hepatocellular carcinoma 1 cm or smaller in patients with chronic liver disease: characterization with gadoxetic acid-enhanced MRI that includes diffusion-weighted imaging. *AJR Am J Roentgenol* 2011; **196**: W758-W765 [PMID: 21606265 DOI: 10.2214/AJR.10.4394]

20 **Witjes CD**, Willemssen FE, Verheij J, van der Veer SJ, Hansen BE, Verhoef C, de Man RA, Ijzermans JN. Histological differentiation grade and microvascular invasion of hepatocellular carcinoma predicted by dynamic contrast-enhanced MRI. *J Magn Reson Imaging* 2012; **36**: 641-647 [PMID:

22532493 DOI: 10.1002/jmri.23681]
21 **Murakami T**, Kim T, Gotoh M, Hasuike Y, Kato N, Miyazawa T, Monden M, Nakamura H. Experimental hepatic dysfunction: evaluation by MR imaging with Gd-EOB-DTPA. *Acad Radiol* 1998; **5** Suppl 1: S80-S82 [PMID: 9561050 DOI: 10.1016/S1076-6332(98)80067-6]
22 **Kim MJ**, Rhee HJ, Jeong HT. Hyperintense lesions on gadoxetate disodium-enhanced hepatobiliary phase imaging. *AJR Am J Roentgenol* 2012; **199**: W575-W586 [PMID: 23096201 DOI: 10.2214/AJR.11.8205]
23 **Hwang HS**, Kim SH, Jeon TY, Choi D, Lee WJ, Lim HK. Hypointense hepatic lesions depicted on gadobenate dimeglumine-enhanced three-hour delayed hepatobiliary-phase MR imaging: differentiation between benignancy and malignancy. *Korean J Radiol* 2009; **10**: 294-302 [PMID: 19412518 DOI: 10.3348/kjr.2009.10.3.294]

P- Reviewers: Liu B, Niu ZS, Xie F **S- Editor:** Wen LL
L- Editor: A **E- Editor:** Ma S

百世登
Baishideng®

Published by **Baishideng Publishing Group Co., Limited**
Flat C, 23/F., Lucky Plaza,
315-321 Lockhart Road, Wan Chai, Hong Kong, China
Fax: +852-65557188
Telephone: +852-31779906
E-mail: bpgoffice@wjgnet.com
http://www.wjgnet.com

ISSN 1007-9327
9 771007 932045